Copper Complexes with New Pyridylpyrazole Based Ligands

by **José A. Campo**[a]), **Mercedes Cano**[a])*, **José V. Heras**[a]), **M. Cristina Lagunas**[a]), **Josefina Perles**[a]), **Elena Pinilla**[a])[b]), and **M. Rosario Torres**[b])

[a]) Departamento de Química Inorgánica I, Facultad de Ciencias Químicas, Universidad Complutense, E-28040 Madrid (e-mail: mmcano@quim.ucm.es)

[b]) Laboratorio de Difracción de Rayos-X, Facultad de Ciencias Químicas, Universidad Complutense, E-28040 Madrid

We report the synthesis, characterization, and crystal structures of new ligands of the pyridinylpyrazole type, *i.e.*, 3,5-bis(4-butoxyphenyl)-1-(pyridin-2-yl)-1*H*-pyrazole (**L^1**) and 3,5-bis(4-phenoxyphenyl)-1-(pyridin-2-yl)-1*H*-pyrazole (**L^2**) (*Scheme 1*), and the study of their coordination behavior towards Cu^I and Cu^{II}. The versatility of this type of ligand, which can give access to different coordination spheres about the metal center, depending on the nature of the copper starting material used in the preparation of the complexes (*Scheme 2*), is illustrated. Thus, pseudo-tetrahedral Cu^I as well as six-coordinated tetragonal and distorted tetragonal pyramidal Cu^{II} derivatives were obtained for $[Cu(L)_2]PF_6$, $[Cu(Cl)_2(L)_2]$ (L = **L^1**, **L^2**), and $[Cu(Cl)(\mathbf{L^1})_2]PF_6$, respectively. We also present a crystallographic support of a distorted octahedral *cis*-bis(tetrafluoroborato-κF)copper(II) compound found for $[Cu(BF_4)_2(\mathbf{L^1})_2]$ (**3**).

Introduction. – Chelating ligands based on the pyrazole ring have been developed extensively in the last years [1][2]. Most of the actual work deals with pyrazole rings bearing one or two bulky N-heterocycle substituents at the 3 and/or 5 position, as this type of ligand often produces multimetallic compounds [1–6]. By constrast, related 1-substituted pyrazoles with heterocyclic substituents, which can act as bidentate ligands, have received less attention [7–9]. They are, however, versatile ligands whose coordinative abilities could be influenced by the nature of additional substituents at the 3 and/or 5 position of the pyrazole ring.

In this context, it is interesting to note that a (pyridinylpyrazole)-type ligand such as 5-methyl-1-(pyridin-2-yl)-1*H*-pyrazole-3-carboxamide (L_c) formed Cu^{II} compounds of formula $[CuX_2(L_c)_2 \cdot H_2O]$ (X= Cl, Br, NO_3, ClO_4) with a distorted octahedral geometry [10]. To achieve that, one of the two L_c ligands acted in a *N*,*N*′-bidentate and the other in a *N*,*N*′,*O*-tridentate fashion with the amide O-atom participating in the latter case and the sixth apical coordination site being occupied by a H_2O molecule or a X counterion [10]. However, a related $[Cu(La)_2]^{2+}$ complex with the 3-(2,5-dimethoxyphenyl)-1-(pyridin-2-yl)-1*H*-pyrazole (L_a) ligand showed a tetrahedrically distorted planar geometry in which, in addition to the CuN_4 core, Cu–O interactions with the MeO groups of each ligand were observed [11].

From these results, it appears that O-containing substituents at the 3 and 5 positions of the pyrazole ring of the pyridinylpyrazole ligands can play an important role in the stereochemistry of the copper derivatives.

Following these precedents, we are now interested in using O-containing 3,5-disubstituted pyridinylpyrazole ligands in metal complexes to produce different geometries that might allow access to certain types of supramolecular arrangements.

For example, if planar molecules can be obtained, then they could be appropriate for columnar stackings interesting for potential liquid-crystal properties.

In this paper, we report the synthesis of two new 1-(pyridinyl)-1*H*-pyrazole ligands (L) bearing bulky and/or long-chain substituents at the 3 and 5 positions of the pyrazole ring, and their reactivity towards Cu^{I} and Cu^{II}. As a result, compounds of general formulae $[Cu(L)_2]PF_6$, $[Cu(X)_2(L)_2]$ (X = Cl or BF_4), and $[Cu(Cl)(L)_2]PF_6$ were prepared. The Cu^{I} derivatives had distorted tetrahedral geometry, but three different geometries were obtained for the Cu^{II} compounds: elongated rhombic octahedral, distorted tetragonal pyramidal, and *cis*-distorted octahedral. While the first one is a common geometry for Cu^{II} complexes, the second and, especially, the third, are less abundant. In the latter, *cis*-coordination of two tetrafluoroborato ligands was found in the solid state and represents the first example of this type of coordination. *Schemes 1* and *2* show the molecular structures of all ligands and compounds synthesized and investigated in this work.

Results and Discussion. – *Synthetic Aspects.* The new bidentate ligands 3,5-bis(4-butoxyphenyl)-1-(pyridin-2-yl)-1*H*-pyrazole (**L¹**) and 3,5-bis(4-phenoxyphenyl)-1-(pyridin-2-yl)-1*H*-pyrazole (**L²**) were obtained by a method analogous to that used in the preparation of related pyridinylpyrazoles (*Scheme 1*) [12][13]. This synthesis requires the condensation of the corresponding 1,3-disubstituted diketone [14] and 2-hydrazinopyridine in EtOH under reflux. However, we observed that the reaction took place to only a very small extent, unless carried out in acidic media. Thus, when acetic or, especially, hydrochloric acid was added, the yield improved significantly. Also, an excess of 2-hydrazinopyridine increased the yield. By contrast, the alternative route which involved reacting the corresponding 3,5-disubstituted 1*H*-pyrazole with potassium hydride and 2-bromopyridine was unsuccessful.

Reaction of **L¹** or **L²** with $[Cu(MeCN)_4]PF_6$ [15] in a 2:1 molar ratio in MeCN (*Scheme 2*) gave the complexes $[Cu(L)_2]PF_6$ **1a** (L = **L¹**) and **1b** (L = **L²**), respectively,

Scheme 1. *Synthesis of Ligands* **L¹** *and* **L²**

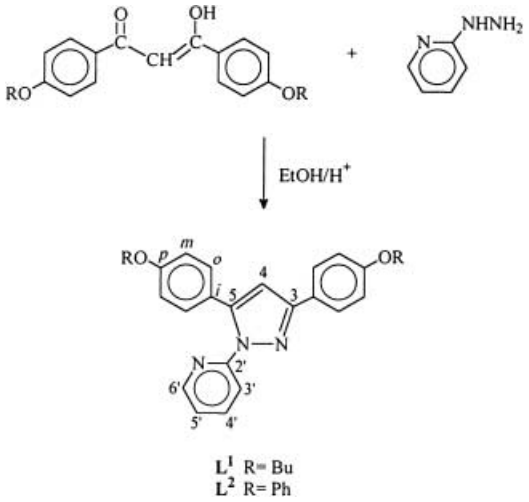

L¹ R = Bu
L² R = Ph

Scheme 2. *Synthesis of Complexes* **1**–**4**

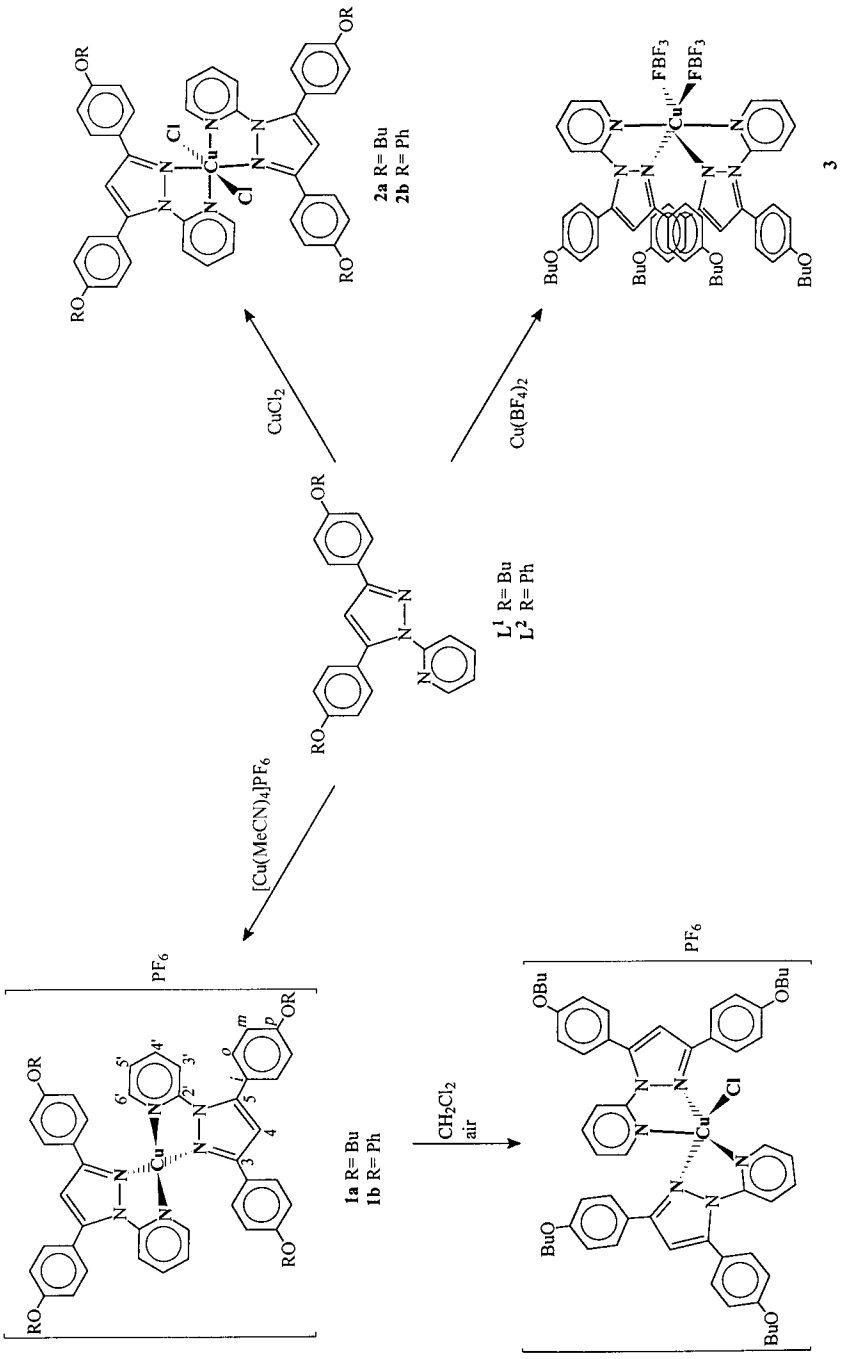

which had distorted tetrahedral geometries as established by X-ray-diffraction analysis. When **L¹** or **L²** was reacted with $CuCl_2 \cdot 2\,H_2O$, in a 2:1 molar ratio and in EtOH/H_2O 50:1 (*Scheme 2*), distorted octahedral complexes of the type *trans*-[$Cu(Cl)_2(L)_2$] **2a** (L = **L¹**) and **2b** (L = **L²**) were obtained, as deduced from X-ray studies. Gentle heating of the reaction mixtures resulted in a faster formation of the above complexes, probably due to complete dissolution of the starting pyridinylpyrazoles. These results encouraged us to try to produce the square planar configuration around the Cu^{II} centre. Thus, given the low tendency of the BF_4^- anion toward σ-coordination [16], the reaction of $Cu(BF_4)_2 \cdot x\,H_2O$ with **L¹** in MeCN in a 2:1 molar ratio was used as synthetic route. But instead of the expected tetracoordinated planar complex, the new octahedral derivative *cis*-[$Cu(FBF_3)_2$(**L¹**)$_2$] **3** was obtained (*Scheme 2*).

Copper(I) complexes **1a** and **1b** are rather stable both as solids and in solutions of nonhalogenated solvents, such as EtOH, MeCN, or acetone. However, in solution of CH_2Cl_2, $CHCl_3$, or CCl_4, formation of traces of Cu^{II} impurities was indicated by ^{1}H-NMR spectroscopy (*i.e.*, signal broadening occurred). An accompanying color change from orange to green was also observed. During this process, which is fastest in the case of **1a**, coordination of chloride to the metal seems likely to take place. In an attempt to characterize the oxidation product, a solution of **1a** in CH_2Cl_2 was left to evaporate slowly in air, which gave a mixture of red and green crystals. While the red crystals were identified as the starting complex **1a**, X-ray studies of the green species confirmed the formation of the pentacoordinated Cu^{II} derivative [Cu(Cl)(**L¹**)$_2$]PF_6 **4**. No further attempts to isolate complex **4** were made.

Spectroscopic and Conductivity Studies. Solid-state IR spectra of all the compounds show $\tilde{\nu}$(CN) absorptions around 1600 cm^{-1}, together with other bands attributable to the pyridinylpyrazole groups. As general feature, the complexes show shifts and/or splitting in some of the characteristic bands with respect to the free ligand. For instance, the γ(CH) vibration is always slightly shifted to higher frequencies. On the other hand, three intense $\tilde{\nu}$(C=C) bands are observed in the region 1500 – 1440 cm^{-1}, in contrast to the complicated pattern of bands exhibited by the free ligands.

Complexes **1a** and **1b** also display absorptions corresponding to the PF_6^- anion ($\tilde{\nu}$(PF) and δ(FPF) at *ca.* 840 and 557 cm^{-1}, resp.), and for the complex **3** bands due to BF_4^- are also observed. The $\tilde{\nu}$(BF) vibration is clearly split into three peaks at 977, 1029, and 1064 cm^{-1}, in contrast to the broad single band centered at 1070 cm^{-1} for the tetrahedral symmetry of the 'free' BF_4^- anion [17]. This splitting indicates a reduction of symmetry of the anions by complex formation, as has already been observed in other complexes containing coordinated BF_4^- anions [17 – 19]. In addition, coordination of the BF_4^- anions in the solid state was also supported by the X-ray-diffraction study of the dark orange crystals of **3** (see below).

The molar conductivities in acetone solution of **1a** and **1b** show them to be 1:1 electrolytes, while values of 20.8 and 21.1 $ohm^{-1}\,cm^2\,mol^{-1}$ for **2a** and **2b**, respectively agree with the neutral nature of the complexes but suggest some degree of dissociation of the chloride ligands in acetone solution. The molar conductivity of 197 $ohm^{-1}\,cm^2mol^{-1}$ for **3** indicates an extensive dissociation of the BF_4^- ions in acetone solution.

^{1}H- and ^{13}C-NMR spectroscopy was used to characterize **L¹**, **L²**, **1a**, and **1b** in solution, while for the paramagnetic complexes **2a**, **2b**, and **3** it was avoided. Although the complexity of the spectra prevented, in some cases, their full assignment, they are in

good agreement with the proposed structures. Thus, the spectra of the four compounds reveal inequivalence of the substituents at the 3 and 5 positions of the pyrazole rings, in accord with the lack of symmetry in the ligands. In the copper complexes **1a** and **1b**, both pyridinylpyrazole ligands are equivalent, *i.e.*, each complex gives a unique group of signals assignable to the H–C(3′) to H–C(6′) of the two pyridinyl substituents and a *s* for H–C(4) of both pyrazole rings.

Another common feature in the NMR spectra of both complexes are the shifts observed for some signals upon coordination. Thus, the pyridine protons are shifted downfield (*i.e.*, H–C(6′) appears at *ca*. 8.42 ppm for $\mathbf{L^1}$ and $\mathbf{L^2}$, and at *ca*. 8.66 ppm for the corresponding complexes **1a** and **1b**). On the other hand, H–C(4) is shifted downfield, and both upfield and downfield shifts are observed for the substituents at the positions 3 and 5 of the pyrazole group of **1a** and **1b** when compared with those of the free ligands. An analogous situation was found for ruthenium complexes containing related pyridinylpyrazole-type ligands, the downfield shifts occurring for pyrazole protons and for the substituents at the 4 and 5 positions, which were attributed to ligand-to-metal σ-donation, whereas upfield shifts for substituents at the 3 position may be ascribed to ring current anisotropy effects [7][12][20–22].

Magnetic Behavior of **2a**, **2b**, *and* **3**. Paramagnetism of complexes **2a**, **2b**, and **3** was clearly evidenced by the magnetic susceptibilities found in the range 2–300 K. In all cases, the *Curie* law was obeyed, and the corresponding magnetic moment values of 1.83, 1.84, and 1.62 MB, respectively, are in the expected range for a Cu^{II} ion ($S = 1/2$) with isolated spins [14][23][24].

X-Ray Structures of $\mathbf{L^1}$, $\mathbf{L^2}$, **1a**, **1b**, **2a**, **3**, *and* **4**. The solid-state structures of the copper compounds **1a**, **1b**, **2a**, **3**, and **4** and of the ligands $\mathbf{L^1}$ and $\mathbf{L^2}$ were determined by single-crystal X-ray diffraction. Selected bond distances and angles are listed in *Tables 1–3*. The best planes formed by the atoms in each of the aromatic rings

Table 1. *Selected Bond Distances* [Å] *and Angles* [°] *for the Ligands* $\mathbf{L^1}$ *and* $\mathbf{L^2}$

L^1			
N(1)–N(2)	1.372(3)	N(2)–C(6)	1.417(4)
N(1)–C(5)	1.329(3)	C(6)–N(3)	1.317(3)
C(5)–C(4)	1.410(4)	C(5)–C(21)	1.463(4)
C(4)–C(3)	1.366(4)	C(3)–C(11)	1.465(4)
N(2)–C(3)	1.382(4)		
N(1)–N(2)–C(3)	111.9(2)	C(5)–N(1)–N(2)	105.5(2)
N(2)–C(3)–C(4)	104.9(3)	N(1)–N(2)–C(6)	117.0(2)
C(3)–C(4)–C(5)	107.7(3)	N(2)–C(6)–N(3)	117.0(3)
C(4)–C(5)–N(1)	110.0(2)		
L^2			
N(1)–N(2)	1.368(3)	N(2)–C(30)	1.430(3)
N(1)–C(5)	1.331(3)	C(30)–N(3)	1.325(3)
C(5)–C(4)	1.409(3)	C(5)–C(18)	1.468(3)
C(4)–C(3)	1.362(3)	C(3)–C(6)	1.478(3)
N(2)–C(3)	1.370(3)		
N(1)–N(2)–C(3)	112.0(2)	C(5)–N(1)–N(2)	104.9(2)
N(2)–C(3)–C(4)	105.8(2)	N(1)–N(2)–C(30)	118.9(2)
C(3)–C(4)–C(5)	106.6(3)	N(2)–C(30)–N(3)	114.9(2)
C(4)–C(5)–N(1)	110.7(2)		

Table 2. *Selected Bond Distances* [Å] *and Angles* [°] *for* $[Cu(L)_2]PF_6$ **1a** (L = **L¹**), *and* **1b** (L = **L²**)

1a			
Cu(1)–N(1)	2.028(7)	Cu(1)–N(4)	2.021(8)
Cu(1)–N(3)	2.035(7)	Cu(1)–N(6)	1.998(7)
N(1)–N(2)	1.35(1)	N(4)–N(5)	1.38(1)
N(1)–C(5)	1.34(1)	N(5)–C(33)	1.33(1)
C(5)–C(4)	1.42(2)	C(33)–C(32)	1.39(1)
C(4)–C(3)	1.33(2)	C(32)–C(31)	1.39(1)
N(2)–C(3)	1.40(1)	N(4)–C(31)	1.33(1)
N(2)–C(26)	1.43(1)	N(5)–C(54)	1.46(1)
C(26)–N(3)	1.33(1)	C(54)–N(6)	1.34(1)
P–F[a])	1.52(1)		
N(1)–Cu(1)–N(3)	80.2(3)	N(3)–Cu(1)–N(4)	137.3(3)
N(1)–Cu(1)–N(4)	108.9(3)	N(3)–Cu(1)–N(6)	119.6(3)
N(1)–Cu(1)–N(6)	138.7(3)	N(4)–Cu(1)–N(6)	81.6(3)
1b			
Cu(1)–N(1)	2.010(7)	Cu(1)–N(4)	2.061(6)
Cu(1)–N(3)	2.033(7)	Cu(1)–N(6)	1.987(6)
N(1)–N(2)	1.39(1)	N(4)–N(5)	1.38(1)
N(1)–C(5)	1.36(1)	N(5)–C(35)	1.39(1)
C(5)–C(4)	1.40(1)	C(35)–C(36)	1.36(1)
C(4)–C(3)	1.34(1)	C(36)–C(37)	1.37(1)
N(2)–C(3)	1.40(1)	N(4)–C(37)	1.35(1)
N(2)–C(30)	1.43(1)	N(5)–C(62)	1.41(1)
C(30)–N(3)	1.29(1)	C(62)–N(6)	1.35(1)
P–F[a])	1.55(7)		
N(1)–Cu(1)–N(3)	80.6(3)	N(3)–Cu(1)–N(4)	131.7(3)
N(1)–Cu(1)–N(4)	114.2(3)	N(3)–Cu(1)–N(6)	120.3(3)
N(1)–Cu(1)–N(6)	137.8(3)	N(4)–Cu(1)–N(6)	80.5(3

[a]) Average of all P–F distances.

were calculated, and the dihedral angles between adjacent rings are discussed below.

In each of the free ligands **L¹** and **L²** (*Figs. 1* and *2*, resp.), both N-donor atoms N(1) and N(3) present an *anti* disposition, possibly due to repulsion between their respective lone pairs as observed in related derivatives [25], but in the copper complexes, they adopt a *syn* conformation necessary for a chelation (see below, *Figs. 3–7*).

In the complexes **1a** or **1b**, the geometry about the metal atom is distorted tetrahedral (*Figs. 3* and *4*), this feature being attributed to the restricted bite angles of the ligands (average 80.9(3) and 80.6(3)° for **1a** and **1b**, resp.). The Cu–N bond distances range between 1.987(6)–2.061(6) Å, as also observed in related Cu^I compounds [11][26][27] (*Table 2*). The coordination planes defined by Cu(1)–N(1)–N(3) and Cu(1)–N(4)–N(6) adopt dihedral angles of 66.3(3) (**1a**) or 72.9(2)° (**1b**), which indicate some deviation from the ideal tetrahedral geometry towards planarity (values between 49 and 89° have been reported for related tetrahedral $[CuL_2]^+$ species [28–31]). Although a more flattened geometry around the metal is a desirable characteristic for adequate stacking, this feature is not achieved in compounds **1a** and **1b**. Thus, the dihedral angles between the least-squares planes of the pyrazol and the adjacent benzene rings for **1a** and **1b** are within the range 12.5(3)–

Table 3. *Selected Bond Distances* [Å] *and Angles* [°] *for [Cu(X)$_2$(**L^1**)$_2$]* **2a** (X= Cl) *and* **3** (X= BF_4), *and [Cu(Cl)(**L^1**)$_2$]PF_6* **4**

2a			
Cu(1)–N(1)	2.643(2)	C(5)–C(4)	1.410(4)
Cu(1)–N(3)	2.019(2)	C(4)–C(3)	1.369(4)
Cu(1)–Cl(1)	2.2817(7)	N(2)–C(3)	1.368(3)
N(1)–N(2)	1.373(3)	N(2)–C(26)	1.409(4)
N(1)–C(5)	1.335(4)	C(26)–N(3)	1.337(5)
N(1)–Cu(1)–N(3)	71.13(8)	N(3)–Cu(1)–Cl(1)	90.32(7)
N(1)–Cu(1)–Cl(1)	87.93(5)	N(3)–Cu(1)–Cl(1A)	89.68(7)
N(1)–Cu(1)–Cl(1A)	92.07(5)	N(1)–Cu(1)–N(3A)	108.87(8)
3			
Cu(1)–N(1)	2.11(1)	Cu(1)–N(4)	2.15(1)
Cu(1)–N(3)	1.96(1)	Cu(1)–N(6)	1.98(1)
Cu(1)–F(1)	2.07(1)	Cu(1)–F(5)	2.07(1)
N(1)–N(2)	1.37(1)	N(4)–N(5)	1.38(1)
N(1)–C(5)	1.36(2)	N(5)–C(33)	1.37(2)
C(5)–C(4)	1.39(1)	C(33)–C(32)	1.41(2)
C(4)–C(3)	1.35(2)	C(32)–C(31)	1.40(2)
N(2)–C(3)	1.37(2)	N(4)–C(31)	1.32(2)
N(2)–C(26)	1.40(2)	N(5)–C(54)	1.32(1)
C(26)–N(3)	1.34(2)	C(54)–N(6)	1.32(1)
B–F[a])	1.41(1)		
N(1)–Cu(1)–N(3)	78.8(5)	N(3)–Cu(1)–N(4)	101.3(4)
N(1)–Cu(1)–N(4)	109.2(4)	N(3)–Cu(1)–N(6)	179.5(5)
N(1)–Cu(1)–N(6)	101.7(4)	N(3)–Cu(1)–F(1)	89.9(5)
N(1)–Cu(1)–F(1)	93.3(5)	N(3)–Cu(1)–F(5)	90.8(5)
N(1)–Cu(1)–F(5)	153.6(5)	N(6)–Cu(1)–F(1)	89.9(5)
N(4)–Cu(1)–N(6)	78.7(4)	N(6)–Cu(1)–F(5)	88.7(5)
N(4)–Cu(1)–F(1)	156.4(5)	F(1)–Cu(1)–F(5)	62.2(6)
N(4)–Cu(1)–F(5)	96.6(5)		
4			
Cu(1)–N(1)	2.053(8)	Cu(1)–N(4)	2.268(7)
Cu(1)–N(3)	1.981(8)	Cu(1)–N(6)	1.997(8)
Cu(1)–Cl(1)	2.275(3)	N(4)–N(5)	1.38(1)
N(1)–N(2)	1.40(1)	N(5)–C(33)	1.39(1)
N(1)–C(5)	1.32(1)	C(33)–C(32)	1.34(1)
C(5)–C(4)	1.43(1)	C(32)–C(31)	1.40(1)
C(4)–C(3)	1.35(1)	N(4)–C(31)	1.36(1)
N(2)–C(3)	1.38(1)	N(5)–C(54)	1.40(1)
N(2)–C(26)	1.41(1)	C(54)–N(6)	1.35(1)
C(26)–N(3)	1.35(1)	P–F[b])	1.55(8)
N(1)–Cu(1)–N(3)	79.6(3)	N(3)–Cu(1)–N(4)	106.2(3)
N(1)–Cu(1)–N(4)	102.4(3)	N(3)–Cu(1)–N(6)	176.5(3)
N(1)–Cu(1)–N(6)	97.8(3)	N(3)–Cu(1)–Cl(1)	93.4(3)
N(1)–Cu(1)–Cl(1)	155.0(2)	N(4)–Cu(1)–N(6)	76.5(3)
N(6)–Cu(1)–Cl(1)	88.0(2)	N(4)–Cu(1)–Cl(1)	102.6(2)

[a]) Average of all B–F distances. [b]) Average of all P–F distances.

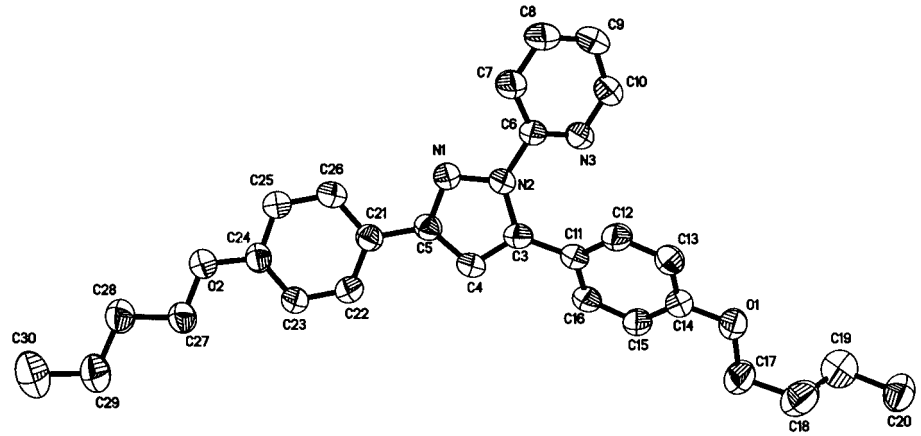

Fig. 1. *Perspective ORTEP of* $\mathbf{L^1}$, *showing the atomic numbering scheme.* H-Atoms are omitted for clarity, and thermal ellipsoids are at 50% probability level.

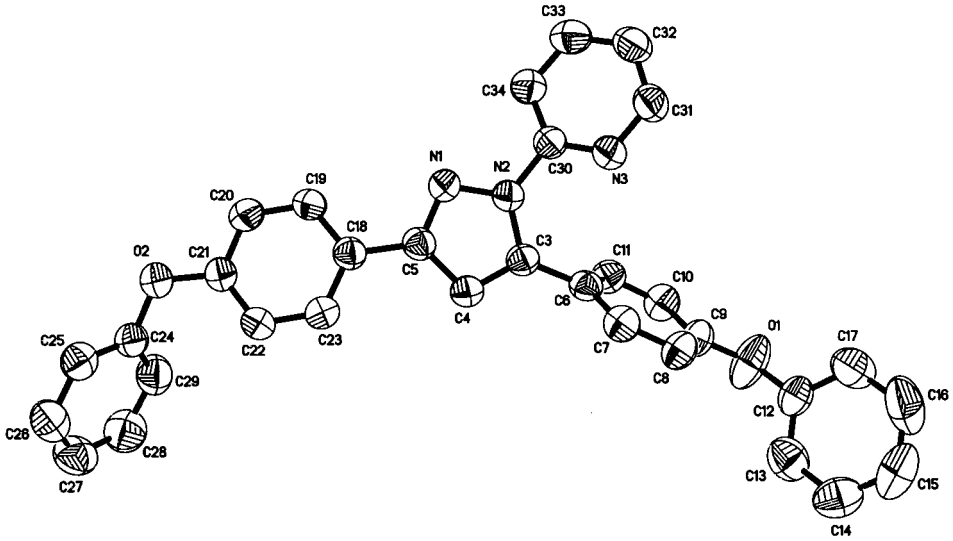

Fig. 2. *Perspective ORTEP of* $\mathbf{L^2}$. Details as in *Fig. 1.*

61.2(3) and 11.1(3)–46.1(3)°, respectively, and for the free ligands, these angles are 5.2(1) and 43.7(1)° in the case of $\mathbf{L^1}$ and 19.0(1) and 68.2(1)° in the case of $\mathbf{L^2}$, whereby the larger angles correspond in all cases to the substituents at the 5 position, this being due to possible steric interactions with the pyridine ring. In addition, adjacent benzene rings in **1b** and $\mathbf{L^2}$ form dihedral angles which lie within 58.1(4)–73.1(4)° and *ca.* 73°, respectively, thus contributing to a lower degree of planarity in these compounds.

Copper(II) complex **2a** shows elongated rhombic octahedral coordination (pseudo-*Jahn-Teller* distortion), with the Cu^{II} ion lying on a crystallographic inversion center (*Fig. 5*). The in-plane Cu–Cl and Cu–N(py) bond lengths are 2.282(1) and

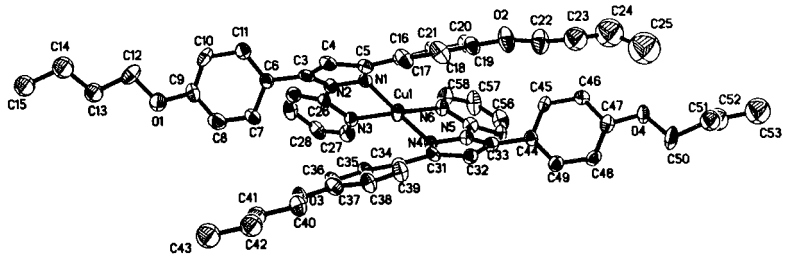

Fig. 3. *Perspective ORTEP of* **1a**, *showing the atomic numbering scheme.* Some atom labels, H-atoms, and the PF_6^- anion are omitted for clarity, and thermal ellipsoids are at 30% probability level.

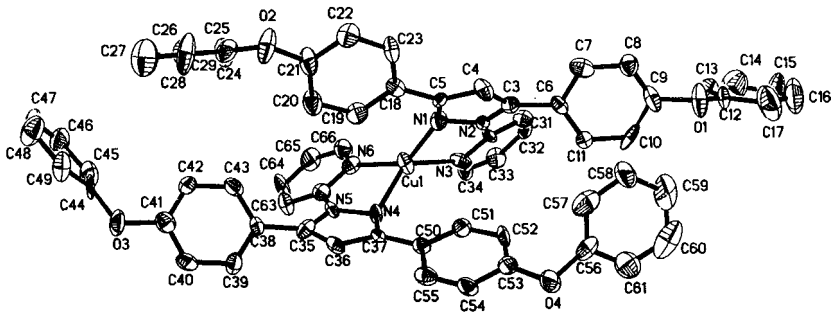

Fig. 4. *Perspective ORTEP of* **1b**. Details as in *Fig. 3*.

2.019(2) Å, respectively (*Table 3*), the latter being comparable to the Cu–N bond distances in complex **1a**. The rhombic distortion of *ca.* 0.3 Å arises from the different covalent radii of the N and Cl ligands [24]. The out-of-plane Cu–N(pz) bond lengths of 2.643(2) Å are significantly longer, giving a tetragonality *T* of 0.76 (*T* = mean in-plane Cu–N distances/mean out-of plane Cu–N distances [32]). The bite angle of the ligand in **2a** (71.13(8)°) is slightly smaller than those in **1a** and **1b**, and the dihedral angles between the pyrazole ring and each of the phenyl substituents at 3 and 5 position (48.3(1)° and 8.2(1)°) are closely related to those in $\mathbf{L^1}$ and $\mathbf{L^2}$ and the Cu^I compounds **1a** and **1b**. However, the pyridine-pyrazole angle is significantly larger (40.3(1)°), probably to minimize repulsions between the pyridine and both the Cl ligands and the substituents at the pyrazole moiety.

The geometry around Cu^{II} in complex **4** can be described as tetragonal pyramidal, heavily distorted towards a trigonal bipyramid (*Fig. 6*). The metal is coordinated to Cl and two pyridinylpyrazole units, with the apical position occupied by the pyrazole N(4) atom. The N(4)–Cu(1)–N(1), N(4)–Cu(1)–N(3), and N(4)–Cu(1)–Cl(1) angles are close to the ideal value of 90° (*Table 3*), but the related N(4)–Cu(1)–N(6) one is smaller (76.5(3)°), this result arising from the chelating nature of the ligand involved. The Cu-center is displaced 0.286 Å from the best least-square plane defined by the atoms Cl(1), N(3), N(1), and N(6). The N(1)–Cu(1)–N(6), N(6)–Cu(1)–Cl(1), N(3)–Cu(1)–Cl(1), and N(1)–Cu(1)–N(3) angles of 97.8(3), 88.0(2), 93.4(3), and 79.6(3)°, respectively, slightly deviate from the ideal value of 90°, again the higher deviation being due to the restricted bite angle of the chelating ligand. By considering

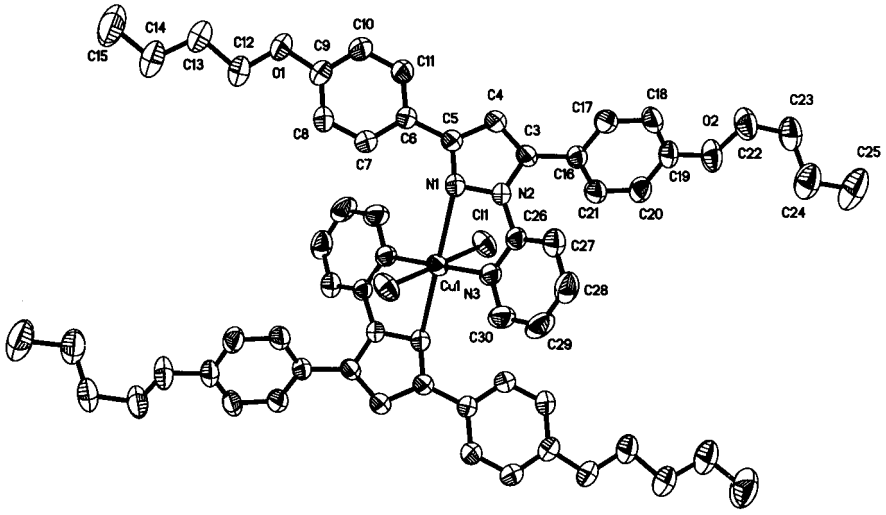

Fig. 5. *Perspective ORTEP of* **2a**, *showing the atomic numbering scheme.* H-Atoms are omitted for clarity, and thermal ellipsoids are at 50% probability level.

the N(6)–Cu(1)–N(3) angle of 176.5(3)°, an alternative geometry around the Cu-center could be a distorted trigonal bipyramid in which the Cu-center is included in the equatorial plane defined by Cl(1), N(1), and N(4). However, the N(1)–Cu(1)–Cl(1) angle of 155.0(2)° is closer to 180° (ideal value in a tetragonal pyramidal geometry) than to 120° (ideal value in a trigonal bipyramidal geometry). Thus, maybe the best would be to suggest a geometry of **4** corresponding to half way between the two possibilities. On the other hand, the same features found in $\mathbf{L^1}$, $\mathbf{L^2}$, **1a**, and **1b** for the dihedral angles between the pyridine and pyrazole rings and between each pyrazole and the aromatic substituent at the 3 and 5 positions are also observed in **4** (the largest angle corresponding to that formed between the pyrazole and the aromatic substituent closer to the pyridine ring). The high *R* values obtained for complexes **1a** and **4** (see below, *Tables 5* and *6*) are due to disorder in the alkyl chains and/or the PF_6^- anion.

The discussion of the crystal-structure resolution of **3** deserves some preliminary comments. Although metal complexes containing BF_4^- as a ligand are not common due to its very weak σ-donor ability [16], some of those containing copper(II) have been described. In these complexes, BF_4^- generally occupies the most remote sites, *i.e.*, the axial positions of either a tetragonal pyramid or a tetragonally elongated octahedron [18][19][33–37], the Cu–F distances being generally considered as arising from weak coordination or semi-coordination [18][19][33–40]. The crystal structure of complex **3** was carried out both at room temperature and low temperature (210 K), but disorder associated with the alkyl chains and the BF_4^- anions prevented better *R* values even after repeated attempts (see below, *Table 6* and *Exper. Part*). However, the data are good enough to suggest a *cis*-distorted octahedral coordination including two chelating ligands and two mono-coordinated FBF_3^- anions in *cis* positions (*Fig. 7*). As it has previously been commented, this feature is not at all common for Cu^{II} complexes and, to our knowledge, complex **3** is the first example of a *cis*-bis(tetrafluoroborato-

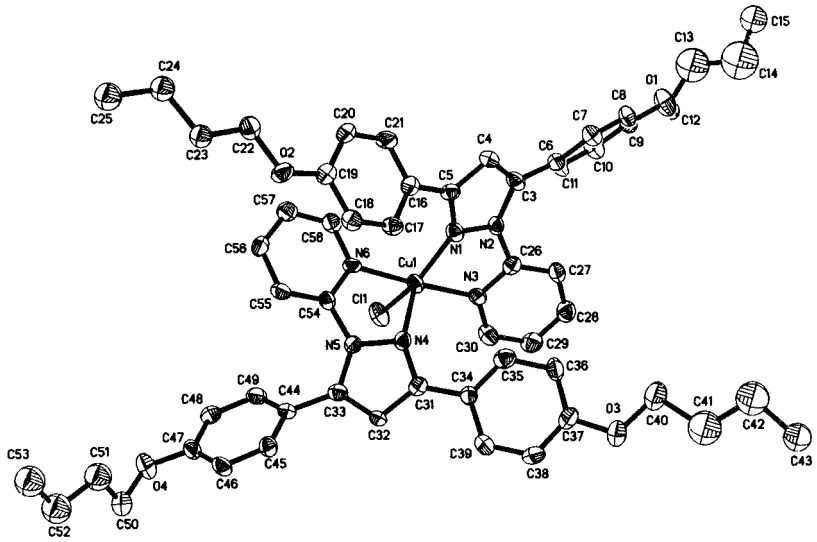

Fig. 6. *Perspective ORTEP of* **4**, *showing the atomic numbering scheme.* H-Atoms and the PF_6^- anion are omitted for clarity, and thermal ellipsoids are at 30% probability level.

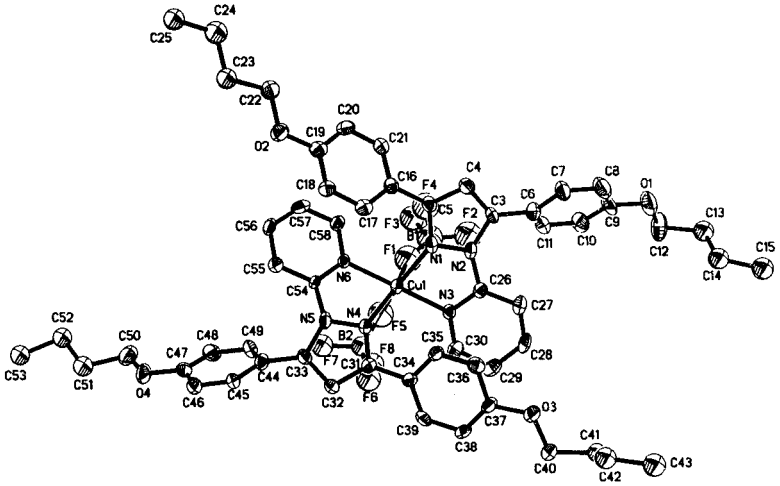

Fig. 7. *Perspective ORTEP of* **3**, *showing the atomic numbering scheme.* H-Atoms are omitted for clarity, and thermal ellipsoids are at 25% probability level.

κF)copper(II) compound. This example opens new expectations for potential starting materials leading to larger aggregates.

Concluding Remarks. – Bidentate (pyridinylpyrazole)-type ligands give rise to homoleptic distorted tetrahedral Cu^I complexes $[CuL_2]^+$, and heteroleptic Cu^{II} distorted octahedral compounds $[Cu(X)_2(L)_2]$ by coordination to CuX_2 fragments.

In addition, halogenated solvents produce the oxidation of a tetrahedral Cu^{I} derivative to give a new compound $[Cu(Cl)(L)_2]^+$ by Cl addition, which presents a tetragonal pyramidal geometry.

The octahedral $[Cu(X)_2(L)_2]$ complexes are found in a *cis* or *trans* coordination depending on the X group (FBF_3 or Cl, resp.). In the former, therefore, the bidentate ligand allows the uncommom coordination of two *cis*-arranged tetrafluoroborato ligands around the Cu^{II} center.

Independently of the geometries found for the complexes, a study of their thermal behavior was carried out by differential scanning calorimetry and polarized-light microscopy. This study was also extended to the free ligands. In all cases, no liquid-crystal behavior was observed. However, the ability of this type of ligand to modulate configurations opens interesting possibilities, and increased efforts should be required to investigate new supramolecular structures.

Experimental Part

General. The starting 1,3-bis(4-butoxyphenyl)propane-1,3-dione and 1,3-bis(4-phenoxyphenyl)propane-1,3-dione were prepared by known methods [14]. The starting Cu^{I} derivative $[Cu(MeCN)_4]PF_6$ was also synthesized by a described procedure [15]. All commercial reagents were used as supplied. Conductivity measurements: *Philips PW9526* conductimeter; *ca.* 10^{-3} M acetone solns.; type of electrolyte determined by comparison with reported data [41]. Magnetic susceptibilities: *SQUID* magnetometer *MPMS XL-5* manufactured by *Quantum Design*, at constant magnetic field of 1 T; 2–300 K temp. range. Melting points: *Olympus BX50* microscope equipped with a *Linkam THMS 600* heating stage; temp. assignment on the basis of visual observations. IR Spectra: *FTIR Nicolet Magna-550* spectrophotometer; KBr discs; 4000–350 cm^{-1} region; in cm^{-1}. ^1H- and $^{13}C\{^1H\}$-NMR Spectra: *Varian VXR-300* (299.88 and 75.40 MHz for ^1H and ^{13}C, resp.) or *Bruker AM-300* (300.13 and 75.43 MHz for ^1H and ^{13}C, resp.) spectrophotometers of the NMR Service of the Complutense University; $CDCl_3$ solns. unless otherwise stated; chemical shifts δ in ppm rel. to $SiMe_4$, with the signal of the deuterated solvent as reference, J in Hz; the atomic numbering according to *Schemes 1* and *2*; accuracy of $\delta(H)$ and $\delta(C)$ ± 0.01 and ± 0.1 ppm, resp., and of J ± 0.3 Hz. FAB-MS: *VG AutoSpec* spectrometer; in *m*/*z*. Elemental analyses (C, H, N) were carried out by the Centre for Elemental Microanalysis of the Complutense University.

*3,5-Bis(4-butoxyphenyl)-1-(pyridin-2-yl)-1*H*-pyrazole* (**L¹**). To a soln. of 1,3-bis(4-butoxyphenyl)propane-1,3-dione (3.68 g, 0.01 mmol) in EtOH (50 ml) was added conc. hydrochloric acid (*ca*. 2.5 ml, spec. grav. 1.18). To this soln., 2-hydrazinopyridine (4.37 g, 0.04 mol) was added slowly, and the yellow soln. was refluxed for 3 h. The solvent was evaporated to *ca*. half the original volume and the resulting soln. kept in a freezer. Colorless needles were formed after 2 days: 3.31 g (75%) of **L¹**. M.p. 88°. ^1H-NMR: 0.98 (*m*, 2 Me); 1.51 (*m*, 2 CH_2); 1.77 (*m*, 2 CH_2); 3.98 (*m*, 2 CH_2O); 6.71 (*s*, H–C(4)(pz)); 6.85 (*d*, $^3J = 9$, 2 H_m); 6.97 (*d*, $^3J = 9$, 2 H_m); 7.21 (*m*, 2 H_o, H–C(5′)(py)); 7.49 (‘*d*’, H–C(3′) (py)); 7.73 (‘*t*’, H–C(4′)(py)); 7.86 (*d*, $^3J = 9$, 2 H_o); 8.42 (‘*d*’, H–C(6′)(py)). ^{13}C-NMR: 13.9 (Me); 19.2, 19.3, 31.2, 31.3 (CH_2); 67.7 (CH_2O); 105.5 (C(4)(pz)); 114.2, 114.5 (C_m); 119.0, 122.1 (C(3′)(py), C(5′)(py)); 125.2, 125.3 (C_i); 127.2, 129.9 (C_o); 138.1 (C(4′)(py)); 144.8, 148.5, 152.4, 152.6 (C(3)(pz), C(5)(pz), C(2′)(py), C(6′)(py)); 159.1, 159.3 (C_p). MS: 442.5 ($[M+H]^+$), 384 ($[M-C_4H_9]^+$), 369 ($[M-C_4H_9O]^+$), 328 ($[M-2C_4H_9]^+$). Anal. calc. for $C_{28}H_{31}N_3O_2$: C 76.16, H 7.08, N 9.50; found: C 76.00, H 7.08, N 9.43.

*3,5-Bis(4-phenoxyphenyl)-1-(pyridin-2-yl)-1*H*-pyrazole (***L²***)*. As described for **L¹**, but starting from the corresponding diketone: 3.5 g (73%) of **L²**. M.p. 126°. ^1H-NMR: 6.77 (*s*, H–C(4)(pz)); 6.96 (*d*, $^3J = 9$, 2 H_m (C_6H_4)); 7.1–7.4 (*m*, 15 H, C_6H_4, C_6H_5O, H–C(5′)(py)); 7.61 (‘*d*’, H–C(3′)(py)); 7.79 (‘*t*’, H–C(4′)(py)); 7.91 (*d*, $^3J = 9$, 2 H_o (C_6H_4)); 8.41 (‘*d*’, H–C(6′)(py)). ^{13}C-NMR: 106.0 (C(4)(pz)); 118.8, 122.3 (C(3′)(py), C(5′)(py)); 118.0, 118.9, 119.0, 199.4 (C_m (C_6H_4), C_m (C_6H_5O)); 123.4, 123.8 (C_p (C_6H_5O)); 125.8, 128.1 (C_i (C_6H_4)); 127.5, 129.8, 129.9, 130.2 (C_o (C_6H_4), C_o (C_6H_5O)); 138.2 (C(4′)(py)); 144.6, 148.4, 152.1, 152.6 (C(3)(pz), C(5)(pz), C(2′)(py), C(6′)(py)); 156.5, 157.1, 157.4, 157.6 (C_p (C_6H_4), C_i (C_6H_5O)). MS: 482 ($[M+H]^+$), 404 ($[M-C_6H_5]^+$), 403 ($[M-C_5H_4N]^+$), 388 ($[M-C_6H_5O]^+$). Anal. calc. for $C_{32}H_{23}N_3O_2$: C 79.81, H 4.81, N 8.73; found: C 79.78, H 5.00, N 8.62.

Bis[3,5-bis(4-butoxyphenyl)-1-(pyridin-2-yl-κN)-1H-pyrazole-κN²]copper(I) Hexafluorophosphate (**1a**). To a soln. of $[Cu(MeCN)_4]PF_6$ (0.08 g, 0.27 mmol) in MeCN (20 ml) was added **L¹** (0.23 g, 0.53 mmol). The resulting suspension was stirred under N_2 and heated gently in a water bath until a reddish orange soln. formed (*ca.* 15 min). This soln. was further stirred at r.t. for 1 h and then evaporated. The resulting red solid was dissolved in EtOH to yield, after slow evaporation, red crystals: 0.13 g (43%) of **1a**. M.p. 197°. Λ_M = 93.2 ohm^{-1}mol^{-1} cm^2. ^{1}H-NMR ($(CD_3)_2CO$): 0.94 (*t*, ^3J = 7, 1 Me); 1.06 (*t*, ^3J = 7, 1 Me); 1.41 (*sext.*, ^3J = 7, 1 CH_2); 1.65 (*m*, 2 CH_2); 1.88 (*qt*, ^3J = 7, 1 CH_2); 3.87 (*t*, ^3J = 7, CH_2O); 4.19 (*t*, ^3J = 7, CH_2O); 6.79 (*d*, ^3J = 9, 2 H_m); 7.05 (*s*, H–C(4)(pz)); 7.21 (*d*, ^3J = 9, 2 H_m); 7.30 ('*d*', H–C(3′)(py)); 7.62 (*m*, 2 H_o, H–C(5′)); 7.74 (*d*, ^3J = 9, 2 H_o); 8.05 ('*t*', H–C(4′)(py)); 8.66 (br. *s*, H–C(6′)(py)). ^{13}C-NMR ($(CD_3)_2CO$): 13.6 (Me); 19.3, 19.4, 31.4, 31.5 (CH_2); 67.7, 68.1 (CH_2O); 109.1 (C(4)(pz)); 114.8, 115.5 (C_m); 116.5, 121.7 (C(3′)(py), C(5′)(py)); 123.0, 123.8 (C_i); 127.8, 130.9 (C_o); 139.7 (C(4′)(py)); 145.8, 148.8, 149.8, 151.2 (C(3)(pz), C(5)(pz), C(2′)(py), C(6′)(py)); 160.5, 161.2 (C_p). Anal. calc. for $C_{56}H_{62}CuF_6N_6O_4P$: C 61.61, H 5.72, N 7.70; found: C 61.56, H 5.97, N 7.64.

Bis[3,5-bis(4-phenoxyphenyl)-1-(pyridin-2-yl-κN)-1H-pyrazole-κN²]copper(I) Hexafluorophosphate (**1b**). As described for **1a**, by starting from **L²**: 0.12 g (38%) of **1b**. Orange crystals. M.p. 182°. Λ_M = 94.5 ohm^{-1} mol^{-1} cm^2. ^{1}H-NMR ($(CD_3)_2CO$): 6.88 (*d*, ^3J = 9, 2 H_m (C_6H_4)); 6.95 (*d*, ^3J = 9, 2 H_m, (C_6H_4)); 7.1–7.6 (*m*, 12 H, C_6H_5O, H–C(4)(pz), H–C(3′)(py)); 7.65 ('*t*', H–C(5′)(py)); 7.67 (*d*, ^3J = 9, 2 H_o (C_6H_4)); 7.84 (*d*, ^3J = 9, 2 H_o (C_6H_4)); 8.08 ('*t*', H–C(4′)(py)); 8.67 ('*d*', H–C(6′)(py)). ^{13}C-NMR ($(CD_3)_2CO$): 109.8 (C(4)(pz)); 116.6, 120.9 (C(3′)(py), C(5′)(py)); 118.6, 119.1, 119.5, 120.0 (C_m (C_6H_4), C_m (C_6H_5O)); 124.3, 124.8 (C_p (C_6H_5O)); 124.2, 125.6 (C_i (C_6H_4)); 128.2, 130.3, 130.6, 131.4 (C_o (C_6H_4), C_o (C_6H_5O)); 139.9 (C(4′)(py)); 145.4, 148.9, 149.5, 150.8 (C(3)(pz), C(5)(pz), C(2′)(py), C(6′)(py)); 156.6, 156.7, 158.8, 159.8 (C_p (C_6H_4), C_i (C_6H_5O)). Anal. calc. for $C_{64}H_{46}CuF_6N_6O_4P$: C 65.61, H 3.96, N 7.71; found: C 65.48, H 4.12, N 7.16.

Bis[3,5-bis(4-butoxyphenyl)-1-(pyridin-2-yl-κN)-1H-pyrazole-κN²]dichlorocopper(II) (**2a**). To a sat. soln. of $CuCl_2 \cdot 2H_2O$ (0.14 g, 0.82 mmol) in EtOH/H_2O 50 : 1 was added **L¹** (0.70 g, 1.6 mmol) and EtOH up to a total

Table 4. *Crystal and Refinement Data for* **L¹** *and* **L²**

	L¹	**L²**
Formula	$C_{28}H_{31}N_3O_2$	$C_{32}H_{23}N_3O_2$
M	441.56	481.53
Crystal system	monoclinic	monoclinic
Space group	$P2_1/n$	$P2_1/n$
a/Å	16.1974(2)	15.2294(1)
b/Å	7.6574(2)	5.7352(1)
c/Å	20.0504(4)	29.1760(6)
β/°	101.324(1)	102.404(1)
U/Å^3	2438.44(9)	2488.85(7)
Z	4	4
F(000)	944	1008
D_c/g cm^{-3}	1.203	1.285
Temp./K	298	298
$\mu(MoK_\alpha)$/mm^{-1}	0.076	0.081
Crystal size/mm	0.40 × 0.20 × 0.15	0.40 × 0.10 × 0.05
Scan technique	ϕ and ω	ϕ and ω
Data collected	(−12, −5, −23) to (19, 9, 22)	(−18, −6, −20) to (17, 6, 34)
θ/°	1.48–25.00	1.40–25.00
Refls. collected	5803	12717
Unique refls.	3997 (R_{int} = 0.029)	4370 (R_{int} = 0.038)
Data, parameters	3997, 298	4370, 335
G.o.f. (F^2)	1.11	1.042
$R(F)$ ($(F^2) > 2\sigma(F^2)$)[a]	0.061 (2357 refls.)	0.053 (2750 refls.)
$wR(F^2)$ (all data)[b]	0.182	0.164
Largest residual peak/e Å^{-3}	0.25	0.26

[a]) $\Sigma[|F_o| - |F_c|]/\Sigma|F_o|$. [b]) $\{\Sigma[w(F_o^2 - F_c^2)^2]/\Sigma[w(F_o^2)^2]\}^{1/2}$.

Table 5. *Crystal and Refinement Data for* **1a** *and* **1b**

	1a	**1b**
Formula	$[C_{56}H_{62}CuN_6O_4]PF_6$	$[C_{64}H_{46}CuN_6O_4]PF_6$
M	1091.63	1171.58
Crystal system	triclinic	orthorhombic
Space group	$P\bar{1}$	$P2_12_12_1$
a/Å	12.452(1)	9.3381(8)
b/Å	13.805(1)	14.811(1)
c/Å	16.312(2)	40.897(4)
α/°	82.562(2)	
β/°	80.978(2)	
γ/°	80.095(2)	
U/Å^3	2712.7(5)	5656.5(9)
Z	2	4
$F(000)$	1140	2408
D_c/g cm^{-3}	1.336	1.376
Temp./K	296	296
$\mu(\text{Mo}K_\alpha)$/mm^{-1}	0.503	0.489
Crystal size/mm	0.15 × 0.15 × 0.15	0.20 × 0.17 × 0.06
Scan technique	ϕ and ω	ϕ and ω
Data collected	(−14, −9, −19) to (14, 16, 19)	(−12, −19, −52) to (11, 17, 53)
θ/°	1.51–25.00	1.46–28.00
Refls. collected	12286	28472
Unique refls.	8180 (R_{int} = 0.0481)	11713 (R_{int} = 0.1117)
Data, restraints, parameters	8180, 2, 559	11713, 0, 703
G.o.f. (F^2)	1.026	0.738
$R(F)$ ((F^2) > 2σ(F^2))[a])	0.11 (3426 refls.)	0.063 (3133 refls.)
$wR(f^2)$ (all data)[b])	0.33	0.167
Largest residual peak/Å^{-3}	1.38	0.60

[a]) $\Sigma[|F_o|-|F_c|]/\Sigma|F_o|$. [b]) $\{\Sigma[w(F_o^2-F_c^2)^2]/\Sigma[w(F_o^2)^2]\}^{1/2}$.

volume of 10 ml. The resulting suspension was heated gently in a water bath until a green soln. formed. After 10 min, the soln. was concentrated to *ca.* half volume and left in the freezer for 24 h, yielding green needles: 0.32 g (40%) of **2a**. M.p. 133°. Λ_M = 20.8 ohm^{-1} mol^{-1} cm^2. Anal. calc. for $C_{56}H_{62}Cl_2CuN_6O_4$: C 66.10, H 6.10, N 8.26; found: C 65.83, H 6.15, N 8.22.

*Bis[3,5-bis(4-phenoxyphenyl)-1-(pyridin-2-yl-*κN*)-1*H*-pyrazole-*κN^2*]dichlorocopper(II)* (**2b**). As described for **2a**, but starting from **L^2**: 0.54 g (62%) of **2b**. M.p. 122°. Λ_M = 21.1 ohm^{-1} mol^{-1} cm^2. Anal. calc. for $C_{64}H_{46}Cl_2CuN_6O_4$: C 70.04, H 4.25, N 7.66; found: C 69.73, H 4.66, N 7.15.

*Bis[3,5-bis(4-butoxyphenyl)-1-(pyridin-2-yl-*κN*)-1*H*-pyrazole-*κN^2*]bis(tetrafluoroborato-*κF*)-copper(II)* (**3**). To a soln. of $Cu(BF_4)_2 \cdot x\ H_2O$ (0.08 g, 0.27 mmol) in MeCN (20 ml) was added **L^1** (0.24 g, 0.53 mmol). The initially blue soln. became brown after a few min. It was stirred at r.t. for 2 h and then evaporated. The resulting brown solid was dissolved in acetone and this soln. left to crystallize by vapor diffusion of Et_2O, yielding dark orange crystals: 0.19 g (65%) of **3**. M.p. 198°. Λ_M = 197 ohm^{-1} mol^{-1} cm^2. Anal. calc. for $C_{56}H_{62}B_2CuF_8N_6O_4$: C 60.04, H 5.58, N 7.50; found: C 60.31, H 5.77, N 7.51.

Crystal-Structure Determinations. Suitable crystals for X-ray experiments of compounds **L^1**, **L^2**, **1a**, **1b**, **2a**, and **3** were obtained as described above (synthetic methods), and those of *bis[3,5-bis(4-butoxyphenyl)-1-(pyridin-2-yl-*κN*)-1*H*-pyrazole-*κN^2*]chlorocopper(II) hexafluorophosphate* (**4**) were formed by aereal oxidation of a CH_2Cl_2 soln. of **1a** (see *Results and Discussion*).

Data collections were carried out at r.t. on a *Bruker Smart-CCD* diffractometer with graphite-monochromated Mo-*K*α radiation (λ 0.71073 Å) operating at 50 kV and different values of intensity depending on the crystals. In all cases, data were collected over a hemisphere of the reciprocal space by combination of three exposure sets. Each exposure of 20 s covered 0.3° in ω, except for **3**, for which different exposure times were used in different data collections, and the best results, although still not ideal, corresponded to 10 s. The

Table 6. *Crystal and Refinement Data for* **2a**, **3**, *and* **4**

	2a	**3**	**4**
Formula	$C_{56}H_{62}Cl_2CuN_6O_4$	$C_{56}H_{62}B_2CuF_8N_6O_4$	$[C_{56}H_{62}ClCuN_6O_4]PF_6$
M	1017.56	1120.28	1127.08
Crystal system	monoclinic	triclinic	triclinic
Space group	$P2_1/c$	$P\bar{1}$	$P\bar{1}$
a/Å	8.3656(2)	13.334(1)	13.856(1)
b/Å	9.8431(2)	14.178(1)	15.176(2)
c/Å	31.9366(1)	15.556(1)	16.095(2)
α/°		85.912(2)	104.340(2)
β/°	91.419(1)	75.780(2)	112.068(2)
γ/°		80.678(2)	108.032(2)
U/Å^3	2628.96(8)	2811.7(4)	2716.1(4)
Z	2	2	2
$F(000)$	1070	1166	1174
D_c/g cm^{-3}	1.285	1.323	1.378
Temp./K	296	296	296
$\mu(\text{Mo}K_\alpha)$/mm^{-1}	0.568	0.465	0.553
Crystal size/mm	$0.40 \times 0.25 \times 0.10$	$0.30 \times 0.20 \times 0.15$	$0.30 \times 0.11 \times 0.06$
Scan technique	ϕ and ω	ϕ and ω	ϕ and ω
Data collected	$(-8, -11, -36)$ to (9, 11, 37)	$(-13, -16, -18)$ to 15, 16, 16)	$(-13, -18, -19)$ to (16, 14, 18)
θ/°	2.17–25.00	1.35–25.00	1.50–25.00
Refls. collected	13893	14829	14386
Unique refls.	4611 ($R_{int} = 0.0431$)	9776 ($R_{int} = 0.0629$)	9455 ($R_{int} = 0.0697$)
Data, restraints, parameters	4611, 0, 313	9776, 28, 562	9455, 12, 569
G.o.f (F^2)	1.045	1.055	0.881
$R(F)$ ($(F^2) > 2\sigma(F^2)$)[a]	0.0470 (3199 refls.)	0.146 (2859 refls.)	0.094 (2941 refls.)
$wR(F^2)$ (all data)[b]	0.109	0.442	0.293
Largest residual peak/e Å^{-3}	0.20	2.42	1.109

[a]) $\Sigma[|F_o| - |F_c|]/\Sigma|F_o|$. [b]) $\{\Sigma[w(F_o^2 - F_c^2)^2]/\Sigma[w(F_o^2)^2]\}^{1/2}$.

first 50 frames were recollected at the end of the data collection to monitor crystal decay, and no apreciable decay was observed, except for **1a**, which gave 10% decay in the intensities of standard reflections. A summary of the fundamental crystal and refinement data is given in *Tables 4–6* for $\mathbf{L^1}$ and $\mathbf{L^2}$, **1a** and **1b**, and **2a**, **3**, and **4**, resp.

The structures of $\mathbf{L^1}$ and $\mathbf{L^2}$ were solved by direct methods and refined by full-matrix least squares on F^2 [42]. All non-H-atoms were refined anisotropically. H-Atoms were included in calculated positions and refined as riding on their respective C-atoms with the thermal parameter related to the bonded atoms.

For **1a**, **1b**, **2a**, and **4**, the structures were solved by *Patterson* function (Cu-atoms) and conventional *Fourier* techniques, and refined by full-matrix least squares on F^2 [42]. Anisotropic parameters were used in the last cycles of refinement for all non-H-atoms with some exceptions. In the compounds containing the PF_6^- anion (**1a**, **1b**, and **4**), no resolvable positional disorder of the F-atoms was found. For these, the F-atoms were included in two isotropical cycles, and in subsequent cycles their thermal parameters were kept constant. Besides, for **1a** and **4**, an analogous refinement was applied for some C-atoms of the butoxy chains, which were also refined with geometric restraints and a variable common C–C distance. H-Atoms were included in calculated positions and refined as riding on their respective C-atoms. These features led to high R factors for **1a** and **4** (see *Tables 5* and *6*).

Many attempts were made to obtain crystals of **3** of good quality. However, only brown crystals with fibrous character that were polysynthetically twinned could be obtained. In spite of this, we considered it of interest to confirm the coordination of the BF_4^- anions, which have little tendency to act as a ligand due to weak σ-donor

ability [16]. Therefore, data collection and refinement of different crystals was carried out at room temp. or at 210 K. The structure was solved by direct methods and *Patterson* function (Cu-atom), and refined by full-matrix least squares on F^2 [42]. It is worth pointing out that both methods yield exactly the same structural model. We observed significant disorder of the BF_4^- groups bonded to the Cu-atom through one F-atom, as well as disorder in some C-atoms of the butoxy chains. To overcome this problem, data collection was performed at low temp. (210 K), but the refinement was worsened, *i.e.* poorer agreement factors were obtained than those at r.t. Thus, this suggests that the disorder is of positional rather than thermal nature. The refinement at r.t. was carried out both in the centric ($P\bar{1}$) and acentric ($P1$) space groups. Despite having more refinable parameters, the acentric model led to higher agreement factors, and furthermore, the thermal parameters of many atoms became negative. Therefore, we propose a structural model in the centric space group (P-1). The refinement of this model was performed with anisotropic parameters in the last cycles for non-H-atoms, except for the BF_4^- groups and some of the C-atoms of the butoxy chains which were refined by only two isotropic cycles with geometrical restraints and variable common C–C and B–F distances.

The largest residual peaks in the final difference map for **1a**, **1b**, **4**, and **3** are in the vicinity of the F-atoms of the PF_6^- and BF_4^- groups, resp.

Crystallographic data for the structures reported in this paper have been deposited with the *Cambridge Crystallographic Data Centre* as supplementary publication nos. CCDC 167535-167541 for **L**[1], **L**[2], **1a**, **1b**, **2a**, **3**, and **4**, resp.

We thank the *DGES* of Spain (Project No. PB98-0766) for financial support.

REFERENCES

[1] J. Pons, A. Chadghan, J. Casabó, A. Alvarez-Larena, J. F. Piniella, X. Solans, M. Font-Bardia, J. Ros, *Polyhedron* **2001**, *20*, 1029, and ref. cit. therein.
[2] M. Munakata, L. P. Wu, M. Yamamoto, T. Kuroda-Sowa, M. Maekawa, S. Kawata, S. Kitagawa, *J. Chem. Soc., Dalton Trans.* **1995**, 4099, and ref. cit. therein.
[3] J. Pons, X. López, E. Benet, J. Casabó, F. Teixidor, F. J. Sánchez, *Polyhedron* **1990**, *9*, 2839.
[4] J. C. Jeffery, P. L. Jones, K. L. V. Mann, E. Psillakis, J. A. McCleverty, M. D. Ward, C. M. White, *Chem. Commun*. **1997**, 175.
[5] K. L. V. Mann, E. Psillakis, J. C. Jeffery, L. H. Rees, N. M. Harden, J. A. McCleverty, M. D. Ward, D. Gatteschi, F. Totti, F. E. Mabbs, E. J. L. McInnes, P. C. Riedi, G. M. Smith, *J. Chem. Soc., Dalton Trans.* **1999**, 339.
[6] J. S. Fleming, E. Psillakis, J. C. Jeffery, K. L. V. Mann, J. A. McCleverty, M. D. Ward, *Polyhedron* **1998**, *17*, 1705.
[7] N. Chabert-Couchouron, C. Marzin, G. Tarrago, *New J. Chem*. **1997**, *21*, 355.
[8] T. K. Lal, R. Gupta, S. Mahapatra, R. Mukherjee, *Polyhedron* **1999**, *18*, 1743.
[9] L. M. L. Chia, A. E. H. Wheatley, N. Feeder, J. E. Davies, M. A. Halcrow, *Polyhedron* **2000**, *19*, 109.
[10] N. Adhikari, S. Chaudhuri, R. J. Butcher, N. Saha, *Polyhedron* **1999**, *18*, 1323.
[11] M. A. Halcrow, E. J. L. McInnes, F. E. Mabbs, I. J. Scowen, M. McPartlin, H. R. Powell, J. E. Davies, *J. Chem. Soc., Dalton Trans.* **1997**, 4025.
[12] N. Chabert, L. Jacquet, C. Marzin, G. Tarrago, *New J. Chem*. **1995**, *19*, 443.
[13] P. J. Steel, F. Lahousse, D. Lerner, C. Marzin, *Inorg. Chem*. **1983**, *22*, 1488.
[14] J. A. Campo, M. Cano, J. V. Heras, M. C. Lagunas, J. Perles, E. Pinilla, M. R. Torres, *Helv. Chim. Acta* **2001**, *84*, 2316.
[15] G. J. Kubas, *Inorg. Synth.* **1990**, *28*, 68.
[16] S. H. Strauss, *Chem. Rev.* **1993**, *93*, 927.
[17] K. Nakamoto, 'Infrared and Ramon Spectra of Inorganic and Coordination Compounds', 4th edn., Wiley, New York, 1986.
[18] A. S. Batsanov, P. Hubberstey, C. E. Russell, *J. Chem. Soc., Dalton Trans.* **1994**, 3189, and ref. cit. therein.
[19] J. Foley, D. Kennefick, D. Phelan, S. Tyagi, B. Hathaway, *J. Chem. Soc., Dalton Trans.* **1983**, 2333.
[20] C. Marzin, F. Budde, P. J. Steel, D. Lerner, *New J. Chem*. **1987**, *11*, 33.
[21] G. Orellana, C. A. Ibarra, J. Santoro, *Inorg. Chem*. **1988**, *27*, 1025.
[22] P. J. Steel, E. C. Constable, *J. Chem. Soc., Dalton Trans.* **1990**, 1389.
[23] A. B. Blake, J. R. Chipperfield, S. Clark, P. G. Nelson, *J. Chem. Soc.*, *Dalton Trans.* **1991**, 1159.

[24] B. J. Hathaway, 'Comprehensive Coordination Chemistry', Eds. G. Wilkinson, R. D. Gillard, and J. A. McCleverty, Pergamon Press, Oxford, 1987, Vol. 5.
[25] R. J. Lees, J. L. M. Wicks, N. P. Chatterton, M. J. Dewey, N. L. Cromhout, M. A. Halcrow, J. E. Davies, *J. Chem. Soc., Dalton Trans.* **1996**, 4055.
[26] P. C. Healy, L. M. Engelhardt, V. A. Patrick, A. H. White, *J. Chem. Soc., Dalton Trans.* **1985**, 2541.
[27] A. G. Orpen, L. Brammer, F. H. Allen, O. Kennard, D. G. Watson, R. Taylor, *J. Chem. Soc., Dalton Trans.* **1989**, S1.
[28] M. A. Halcrow, N. L. Cromhout, P. R. Raithby, *Polyhedron* **1997**, *16*, 4257.
[29] D. A. Bardwell, A. M. W. Cargill Thompson, J. C. Jeffery, E. E. M. Tilley, M. D. Ward, *J. Chem. Soc., Dalton Trans.* **1995**, 835.
[30] E. Müller, G. Bernardinelli, J. Reedijk, *Inorg. Chem*. **1996**, *35*, 1952.
[31] S. M. Scott, K. C. Gordon, A. K. Burrell, *Inorg. Chem*. **1996**, *35*, 2452.
[32] A. A. G. Tomlinson, B. J. Hathaway, D. E. Billing, P. Nichols, *J. Chem. Soc. A* **1969**, 65.
[33] C. F. Martens, A. P. H. J. Schenning, M. C. Feiters, J. Heck, G. Beurskens, P. T. Beurskens, E. Steinwender, R. J. M. Nolte, *Inorg. Chem*. **1993**, *32*, 3029.
[34] L.-P. Wu, M. E. Keniry, B. Hathaway, *Acta Crystallogr., Sect. C* **1992**, *48*, 35.
[35] A. S. Batsanov, P. Hubberstey, C. E. Russell, P. H. Walton, *J. Chem. Soc., Dalton Trans.* **1997**, 2667.
[36] P. Hubberstey, J. Stroud, *Polyhedron* **1997**, *16*, 3687.
[37] A. J. Blake, P. Hubberstey, W. S. Li, C. E. Russell, B. J. Smith, L. D. Wraith, *J. Chem. Soc., Dalton Trans.* **1998**, 647.
[38] G. J. A. A. Koolhaas, W. L. Driessen, J. Reedijk, J. L. van der Plas, R. A. G. de Graaff, D. Gatteschi, H. Kooijman, A. L. Spek, *Inorg. Chem*. **1996**, *35*, 1509.
[39] C. Hemmert, M. Renz, H. Gornitzka, B. Meunier, *J. Chem. Soc., Dalton Trans.* **1999**, 3989.
[40] B. J. Hathaway, D. E. Billing, *Coord. Chem. Rev.* **1970**, *5*, 143.
[41] W. J. Geary, *Coord. Chem. Rev.* **1971**, *7*, 81.
[42] G. M. Sheldrick, 'SHELXL97, Program for Refinement of Crystal Structure', University of Göttingen, Germany, 1997.

Received October 23, 2001